Impact on Power System Frequency Dynamics from an HVDC Transmission System With Converter Stations Controlled as Virtual Synchronous Machines

Francesco Palombi
Luigi Piegari
Department of Electronics, Information and Bioengineering
Politecnico di Milano
Milano, Italy
luigi.piegari@polimi.it

Salvatore D'Arco
Atsede G. Endegnanew
Jon Are Suul
SINTEF Energy Research,
Trondheim, Norway
Jon.A.Suul@sintef.no

***Abstract*— This paper evaluates the operation of an HVDC interconnection for providing virtual inertia and the impact on the power system frequency dynamics when one or both the converter terminals are controlled as a virtual synchronous machine (VSM). The analysis aims at assessing the performance of the inertia support from a power system perspective by studying the impact on the frequency nadir and the Rate-of-Change-of-Frequency (RoCoF) of two asynchronous power system equivalents. It is demonstrated how the dc voltage control can be integrated with the VSM-based control when both converter terminals should be controlled to provide inertia support, but it is also found that this may require additional capacitance to ensure sufficient stability margins. Simulations in PowerFactory are presented for a case with two asynchronous power system equivalents connected by an HVDC transmission scheme modelled with parameters based on the planned Nordlink connection between Norway and Germany. The results confirm the beneficial effects of the inertia support on the frequency dynamics and demonstrate how the VSM-based control provides a clear improvement of the frequency nadir compared to traditional power-frequency droop control.**

***Index Terms*—Frequency dynamics, HVDC transmission systems, Virtual Inertia, Virtual Synchronous Machines**

I. Introduction

The introduction of large-scale renewable power generation with power electronic interfaces into the power system is leading to reduced equivalent inertia and rising levels of rate-of-change-of-frequency (RoCoF) in response to disturbances [1], [2]. Such conditions are already challenging the operation of islanded systems with high penetration of wind power generation, as in Ireland and in the UK [3], [4]. However, also larger interconnected power systems like the continental European power system are expected to experience periods with reduced equivalent inertia when the renewable power generation will further increase [5]. In the hydro-dominated Nordic power system, challenges related to low inertia operation will occur during low load and high import from existing and future HVDC interconnections with the neighboring power systems [6]. In such conditions, control of the HVDC converters for providing virtual inertia could be an effective measure for increasing the equivalent inertia and improving the frequency dynamics of the power systems.

Several recent publications have proposed to utilize Voltage Source Converter (VSC) HVDC systems for providing virtual inertia. However, many of the proposed control methods utilize the frequency derivative (i.e. the *df/dt* or RoCoF) to calculate the emulated inertial response [7]-[11]. Such control strategies can be easily integrated with conventional VSC control loops but rely on synchronization with a relatively strong grid voltage for the *df/dt* estimation. As an alternative approach for providing virtual inertia, Virtual Synchronous Machines (VSMs) with explicit emulation of a synchronous machine (SM) swing equation have been widely studied for various applications [12]-[15]. Such control strategies rely on the power-balance-based synchronization mechanism of their virtual swing equation, and since they operate in a similar way as SMs, they do not depend on a Phase Locked Loop (PLL) for grid synchronization. Thus, the same operational flexibility as for SMs is ensured, including the ability to operate in strong grids, in stand-alone systems with a local load, or in any intermediate conditions. However, most previous publications on VSM-based control for HVDC applications, as for instance [16]-[18], have studied the implementation and control system performance for individual converter terminals without addressing the impact of the inertia support on realistic network models from a power system perspective. Furthermore, except for some examples in [19], [20], the VSM-based provision of virtual inertia at both sides of a

This work was supported by the project "HVDC Inertia Provision" (HVDC Pro), financed by the ENERGIX program of the Research Council of Norway (RCN) with project number 268053/E20 and the industry partners; Statnett, Statoil, RTE and ELIA.

This is the accepted version of an article published in 2019 IEEE Milan PowerTech
http://dx.doi.org/10.1109/PTC.2019.8810855

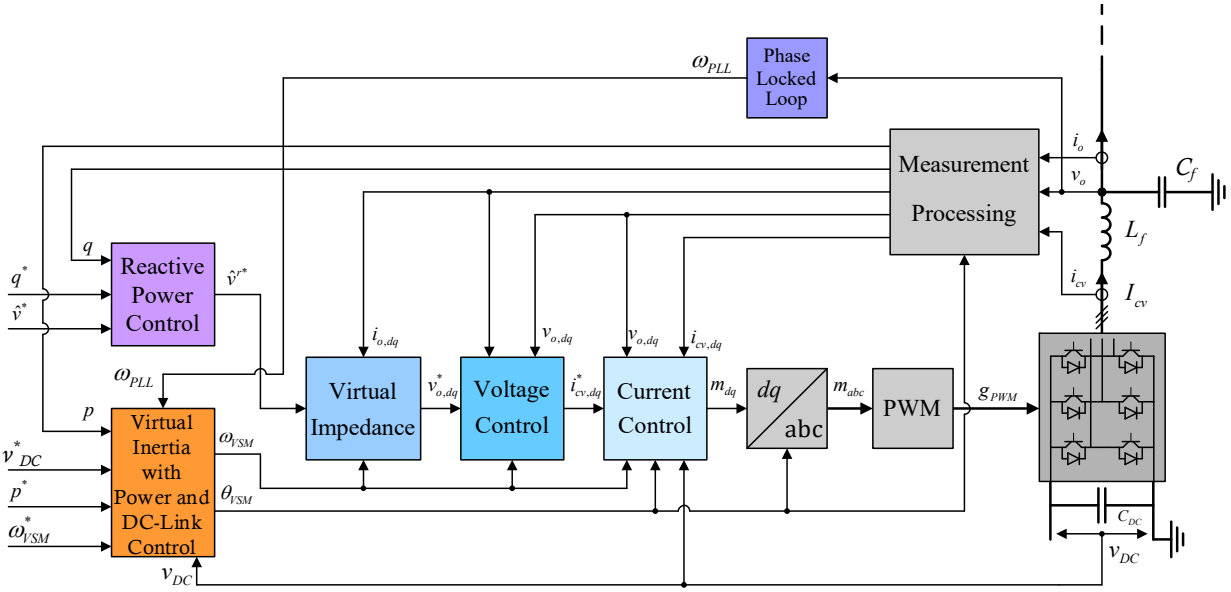

Fig. 1. Overview of the control system for an HVDC converter terminal operated as a Virtual Synchronous Machine

point-to-point HVDC transmission system have not been sufficiently assessed.

This paper studies the utilization of a VSM-based control scheme with cascaded voltage and current controllers in an HVDC interconnection between two asynchronous power systems. The applied control strategy is implemented for a simulation model in PowerFactory which includes the frequency dynamics of simplified power system equivalents on both sides of the HVDC system. It is first demonstrated how VSM-based control in one of the HVDC terminals can provide inertial response and significantly improve the frequency nadir in case of disturbances in the power system. Then, it is shown how a dc-voltage controller can be integrated in the VSM-based control scheme, in order to operate both HVDC converter terminals as VSMs. However, this requires significantly reduced bandwidth of the dc voltage control and depends on a relatively large dc-side capacitance since more energy will be extracted from the dc-system.

II. HVDC CONVERTER CONTROL IMPLEMENTATION

To investigate the impact of VSM-based control on the power system frequency dynamics, two control system configurations of a point-to-point HVDC transmission system are presented in this paper. In the first configuration, one terminal is controlled as a VSM for providing virtual inertia, while the other terminal is controlled with a conventional dc-link voltage controller. In the second configuration, both HVDC converters are controlled as VSMs and provide inertia support to the ac grid. However, the VSM implementation for one of the terminals is slightly modified in order to embed the functionalities of the dc voltage controller.

A. Reference VSM control implementation

The control schemes utilized in this paper are based on the VSM implementation presented in [21]. An overview of the control system for a converter terminal operating as VSM is shown in Fig. 1. The VSM-based inertia emulation provides the frequency ω_{VSM} and the phase angle θ_{VSM}, utilized by the internal control loops, while the reactive power controller provides the voltage amplitude reference $\hat{v}^{r*}$. Hence, the VSM inertia emulation and the reactive power controller appear as outer loops providing references for the cascaded voltage and current controllers. A Phase Locked Loop (PLL) it utilized to detect the actual grid frequency, but this frequency is only used for implementing the damping term in the swing equation. Thus, the inner loop controllers do not rely on the PLL as in a conventional VSC control system, but only on the power balance-based synchronization mechanism of the emulated SM swing equation [21].

A block diagram showing the implementation of the VSM swing equation is shown on the right-hand side of Fig. 2. The swing equation used for the implementation is linearized with respect to the speed so that the acceleration of the inertia is determined by the power balance as

$$s \cdot \omega_{VSM} = \frac{p^{r*}}{T_a} - \frac{p}{T_a} - \frac{p_d}{T_a} \tag{1}$$

where p^{r*} is the virtual mechanical input power, p is the measured electrical power injected into the grid by the VSM, and p_d is the damping power. The mechanical time constant is defined as T_a, corresponding to $2H$ in a traditional SM. The per unit mechanical speed ω_{VSM} of the virtual inertia is given by the integral of the power balance while the corresponding phase angle θ_{VSM} is given by the integral of the speed.

An external frequency droop, equivalent to the steady-state characteristics of the speed governor for a traditional synchronous machine, is included in the power control of the VSM as shown in the lower left side of Fig. 2. This power-frequency droop is characterized by the droop constant k_ω acting on the difference between a frequency reference ω^*_{VSM} and the actual VSM speed ω_{VSM}. Thus, the virtual mechanical input power p^{r*} to the VSM swing equation results from the sum of the external power reference set-point, p^r, and the

This is the accepted version of an article published in 2019 IEEE Milan PowerTech
http://dx.doi.org/10.1109/PTC.2019.8810855

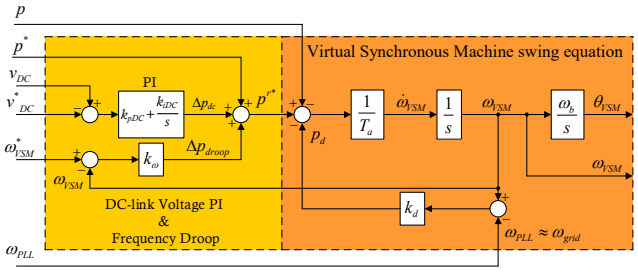

Fig. 2 Virtual Synchronous Machine swing equation with power-frequency droop (section II.B) or dc-voltage controller (section II.C)

frequency droop effect Δp_{droop}. By substituting the droop expression into (1), and expanding the damping term as expressed from the grid frequency detected by the PLL, the virtual swing equation is given by:

$$s \cdot \omega_{VSM} = \frac{p^{r*}}{T_a} - \frac{p}{T_a} - \frac{k_d\left(\omega_{VSM} - \omega_{PLL}\right)}{T_a} - \frac{k_\omega\left(\omega_{VSM} - \omega^*\right)}{T_a} \quad (2)$$

While the instantaneous phase angle θ_{VSM}, utilized in the control system is directly defined in Fig. 2, the phase displacement between the VSM and the equivalent voltage source of a power system model is defined by,

$$s \cdot \delta\theta_{VSM} = \left(\omega_{VSM} - \omega_G\right) \cdot \omega_b \quad (3)$$

where ω_G is the speed of an equivalent generator representing the aggregated inertia of the power system. This phase displacement is needed for synchronous reference frame modelling and small-signal eigenvalue analysis.

B. One HVDC terminal controlled as VSM

As a first case, the inverter terminal is controlled as a VSM while the rectifier terminal is operated with a conventional dc-voltage control strategy with inner loop current controllers as shown in Fig. 3. The d- and q-axis current references are provided by the dc-link voltage control and the ac voltage or reactive power control, respectively. The dc voltage is controlled by a PI controller defined by the proportional and integral gains k_{pDC} and k_{iDC} as:

$$i^*_{cv,d} = \left(k_{pDC} + \frac{k_{iDC}}{s}\right)\left(v_{DC} - v^*_{DC}\right) \quad (4)$$

The current reference from the dc-voltage controller should be limited to avoid over-currents in case of voltage drops, fault conditions or other severe transients. A priority for the direct current has been selected to maintain the dc voltage around the equilibrium point. This also implies that the dc-voltage controller must be protected from windup conditions in case the current reference is saturated [23].

C. Both HVDC terminals controlled as VSM

As described in section II.A, the VSM-based power control with inertia emulation provides the frequency and phase angle references for the inner loop controls, and the reactive power controller provides the reference amplitude of the voltage. Virtual inertia support at both sides of an HVDC interconnection can be obtained by utilizing the same VSM-based control structures for both converter terminals while interfacing a dc-voltage controller with the power balance of the virtual swing equation in one or both the converter stations. In this case, a PI-controller operating on the dc-voltage, as indicated in the upper left part of Fig. 2, is introduced in the converter terminal operating as a rectifier which will be responsible for balancing the dc voltage. The dc-voltage PI controller output Δp_{dc}, will modify he virtual mechanical power input p^{r*} to the swing equation as also indicated in the left of Fig. 2. Thus, the power balance of the VSM inertia with dc-voltage control can be expressed as

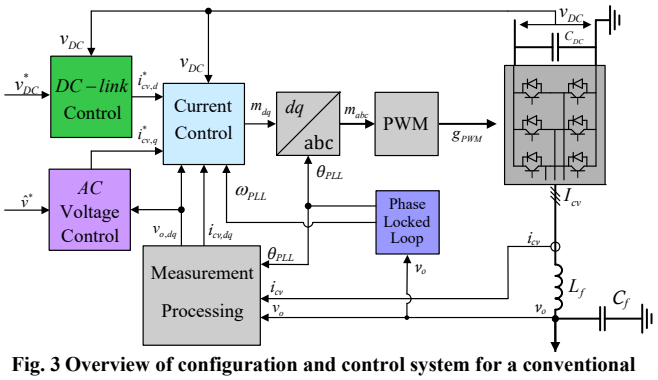

Fig. 3 Overview of configuration and control system for a conventional VSC-based HVDC terminal with dc-link voltage control

$$s \cdot \omega_{VSM} = \frac{p^*}{T_a} - \frac{p}{T_a} - \frac{k_d\left(\omega_{VSM} - \omega_{PLL}\right)}{T_a} + \left(k_{pDC} + \frac{k_{iDC}}{s}\right)\left(v_{DC} - v^*_{DC}\right)\frac{1}{T_a} \quad (5)$$

It should be noted that the frequency droop contribution is not considered and the droop constant k_ω from (2) is set to zero for the terminal controlling the dc voltage. The reason is that the dc-voltage PI controller eliminates steady-state errors and will compensate any steady-state contribution from power frequency droop. However, if the integral part of the dc-voltage is disabled to obtain a droop-based control scheme, multiple terminals could contribute to the dc voltage control as well as to the ac-side frequency control.

III. Simulation Study

This section presents numerical simulation results for a point-to-point HVDC connection, to assess the impact of the VSM-based control on the power system frequency dynamics and the power flow of the HVDC system. The dynamic simulations have been performed with the commercial software DIgSILENT Power Factory. Since the simulations are mainly intended to study the inertial dynamics, the switching effects of the VSC are neglected and ideal average models are assumed for representing the converter terminals.

A. Simulated system configuration

The HVDC interconnection of the simulated system is based on the planned Nordlink interconnector, which will connect the Nordic grid to the Continental Europe (UCTE) power system with a 623 km bipolar HVDC link rated at 1500 MVA and ±525 kV dc [26], [27]. For the simulated case, HVDC converter stations with ratings and parameters corresponding to the Nordlink interconnection are interfaced with two asynchronous areas with a nominal voltage of 285 kV rms (line-to-line) at 50 Hz. These two ac grids are aggregated models composed of a single node with parallel connected synchronous generators and a lumped load, as

This is the accepted version of an article published in 2019 IEEE Milan PowerTech
http://dx.doi.org/10.1109/PTC.2019.8810855

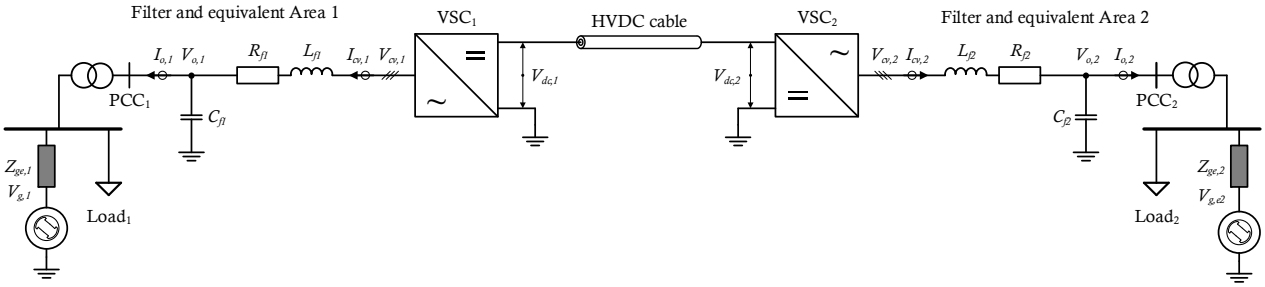

Fig. 4 Overview of investigated system configurations for point-to-point HVDC transmission schemes

TABLE I MAIN SYSTEM PARAMETERS

Parameter	Value	Parameter	Value
Rated voltage $V_{N,LL,rms}$	285 kV	Filter inductance L_{f1},L_{f2}	0.08 pu
Rated power S_b	1.5 GVA	Filter resistance R_{f1},R_{f2}	0.003 pu
Rated angular frequency ω_b	2π*50 Hz	Filter capacitance c_f	0.074 pu
Frequency droop gain, k_ω	20 pu	Filter inductance L_{g1},L_{g2}	0.028 pu
VSM damping factor k_d	300 pu	Filter resistance R_{g1},R_{g2}	0.0008 pu
VSM inertia time constant T_a	20 s	dc side resistance series R_{dc}	0.086 pu
Equivalent dc side capacitance c_{dc} / Equivalent dc-side capacitor charging time T_C			41.28 pu / 100 ms

shown in Fig. 4. The load is represented by a ZIP-model with 10% constant impedance, 30% constant current load and 60% constant power load. Each area contains 24 parallel synchronous machines rated for 250 MVA at 22 kV (line-to-line rms) leading to a total installed capacity of 6000 MVA. For the simulations in PowerFactory, the generators are represented by a 6th order model with default parameter settings, which are equipped with governors, voltage regulators (AVR) and power system stabilizers (PSS). The inertia time constant T_a of both areas is assumed to be 10 s and the steady-state droop gain of the governor is 5%.

The two HVDC converters are connected to their associated asynchronous areas through an *LCL* ac filter. The main parameters of the system configuration and of the VSM-based inertia emulation are reported in Table I. A per unit system based on the rated apparent power of the converter and the peak value of the rated phase voltage is applied for all parameters and simulation results. The parameters of the dq-frame PI current and voltage controllers of the VSMs as well as the conventional control system from Fig. 3 are designed according to the Modulus Optimum (MO) and Symmetrical Optimum (SO) criteria respectively, according to [24],[25] and are not reported in the table for brevity.

The dc cable of the HVDC interconnector has been modelled with a π-model with a single section. As a starting point, the dc bus capacitors of the converter stations were selected to correspond to the equivalent capacitance of a Modular Multilevel Converter (MMC) designed to limit the fundamental frequency sub-module capacitor voltage ripple within 5% [22]. However, for the case of VSM-based control at both sides of the HVDC interconnection, the dc voltage controller must be designed to be slower than the inertial response expected by the converter station at the AC side, to avoid that the two control functions will be conflicting. Furthermore, initial eigenvalue-based analysis of the small-signal dynamics of the case with VSM-based controllers at both sides of the HVDC interconnection, has confirmed how this control configuration will experience stability problems for high values of virtual inertia and/or low values of equivalent dc-side capacitance [28]. In this case, it has been assumed that the VSM inertia constant should be kept at a relatively high value of T_a = 20 s. Therefore, it becomes necessary to introduce a buffer capacitance or a small auxiliary energy storage to support the simultaneous inertia emulation at both sides of the HVDC interconnection. According to the analysis conducted in [28], a total equivalent dc-side capacitance c_{dc} with a charging time T_C in the range of 100 ms will be sufficient for operating the system with reasonable dynamics and stability margins. Thus, the total capacitance c_{dc} used in the simulations includes the equivalent cable capacitance, the equivalent capacitive energy storage of the converter terminal and any additional buffer capacitance required to reach a T_C of 100 ms.

For the simulations presented in the following, the system parameters including the equivalent dc-side capacitance are kept the same for all investigated cases. However, the tuning of the dc voltage controller is adapted to the different cases. The PI controller parameters for the dc voltage controller are set to k_{pDC} = 3 pu and k_{iDC} = 1 pu for the configuration with VSM-based control in one HVDC converter terminal while they are given by k_{pDC} = 2.5 pu and k_{iDC} = 0.67 pu for the case where both converter terminals rely on VSM-based control.

B. Time domain simulation results

The system is assumed to initially operate in steady state conditions corresponding to a power production of each area equal to 80% of the total power capacity, with a power factor of 0.9. Moreover, the interconnector operates with 750 MW power transfer (i.e. 0.5 pu) from Area 2 to Area 1. The power system is then perturbed with a step of 0.1 pu increase in the total ZIP-load of Area 1 at 1 s. The results from this simulation are shown in Fig. 5, where the frequency in Area 1 and Area 2 are given in Fig. 5 a) and b), respectively, while the ac-side power flow from the converter stations in Area 1 and Area 2 are given in Fig. 5 c) and d), respectively. Each plot in the figure shows results from 3 cases, i.e. i) a reference case with conventional control systems, utilizing a conventional power control with a frequency droop in Area 1 and a dc-voltage control according to Fig. 3 for the converter in Area 2, ii) VSM-based control for Area 1 and conventional dc voltage control for the converter in Area 2, and iii) VSM-

This is the accepted version of an article published in 2019 IEEE Milan PowerTech
http://dx.doi.org/10.1109/PTC.2019.8810855

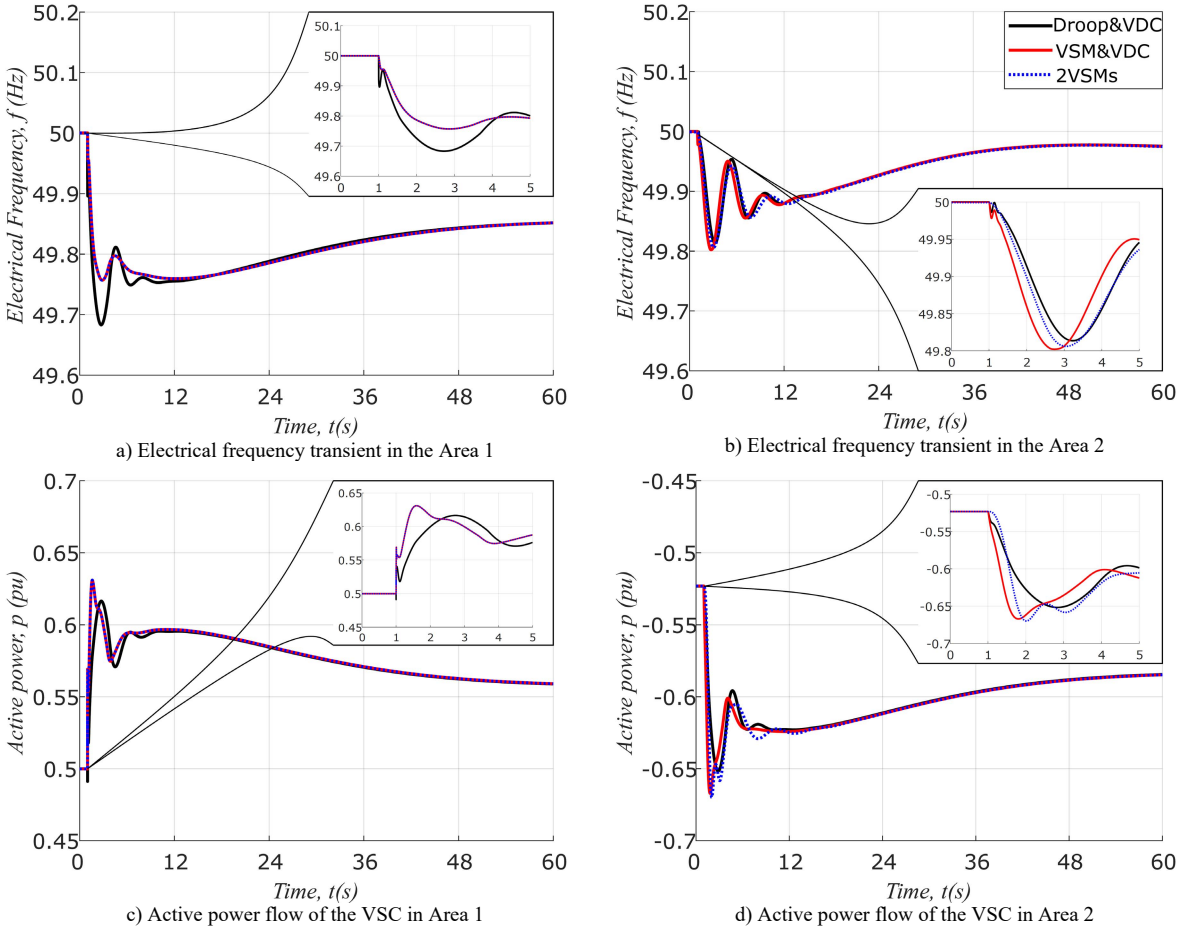

a) Electrical frequency transient in the Area 1

b) Electrical frequency transient in the Area 2

c) Active power flow of the VSC in Area 1

d) Active power flow of the VSC in Area 2

Fig. 5 Transient response of frequency and power flow of converter station for Area 1 and Area 2

based control for both converters, but with dc voltage control by the converter in Area 2. Corresponding results for the dc voltages are shown in Fig. 6.

When the load step occurs, the electrical frequency starts decreasing in both Areas, as shown in Fig. 5 a) and b). From the curves it is clear how the virtual inertia of the VSM-controlled converter terminals contributes to a reduction of the RoCoF immediately after the load step. Furthermore, the figures show how the added virtual inertia helps to improve the frequency nadir. For Area 1, it is also clear from Fig. 5 c) how the reduced RoCoF is obtained by a temporary increase of the power injection from the HVDC terminal.

As expected, the power responses and frequency dynamics of Area 1 is the same for the two cases with VSM-based control. However, the transient response in Area 2 differs noticeably between the three cases during the first 5 seconds after the disturbance, as shown in Fig. 5 b) and d). The difference between the two first cases is mainly caused by the impact on the power transfer from the inertia emulation in Area 1, while the differences between case ii) and case iii) are associated with the introduction of the virtual inertia in Area 2 as well as the change in the control of the dc-link voltage. In particular, the increase of power flow into the HVDC terminal of Area 2 in response to the load change in Area 1 is delayed for the case with two VSMs. This implies that more energy is

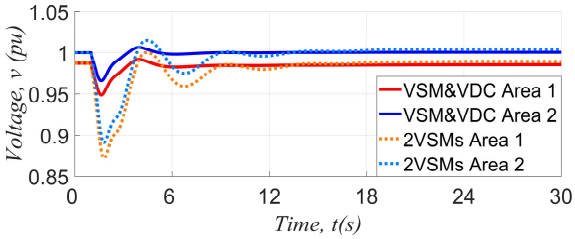

Fig. 6 DC voltage transient response

transiently extracted from the dc-system compared to the case with only one VSM-controlled converter station. The corresponding dc voltage transients at both ends of the dc cable are clearly seen in Fig. 6. The increased exploitation of the energy stored in the dc system is delaying the frequency nadir of Area 2 compared to case ii). This is also the reason why additional buffer capacitance was needed to maintain reasonable dynamics and stability margins when operating with a dc-voltage controller cascaded with one of the VSM-based control systems. Still, the results show that with the same system parameters, the RoCoF is slightly reduced and the frequency nadir in Area 2 is slightly improved for the case of two VSMs compared to the configuration with only one VSM, even if the maximum power flow of the HVDC terminal in Area 2 is increased. However, it should be noted that the case with traditional droop control has the best dynamic response with the less severe frequency nadir in Area

This is the accepted version of an article published in 2019 IEEE Milan PowerTech
http://dx.doi.org/10.1109/PTC.2019.8810855

2. This is proved by the fact that the inertia emulation increases the power injection on the Area 1 and consequently perturbs the dc voltage more than the traditional droop control due to the sharing of the inertia between the two systems. Compared to the reference case, the operation with two VSMs is causing higher variations in the power flow but only a marginally worse frequency nadir and a slightly more damped frequency oscillation with a longer settling time.

IV. Conclusion

The control of HVDC converter stations as Virtual Synchronous Machines (VSMs) can be an effective approach for inertia provision and for mitigating future challenges associated with low physical inertia in the transmission system. In this paper, two alternative controller configurations for an HVDC interconnection have been presented and assessed in comparison to a conventional benchmark case with a frequency droop in the power-controlled converter terminal. In the first configuration, one of the HVDC converter terminals is operated as a VSM to provide virtual inertia to the ac power system while a standard dc voltage control is utilized at the other converter terminal. The second alternative demonstrates how both converter stations can be controlled as VSMs, by integrating the dc-voltage controller with the power reference for the VSM control at one side of the interconnection. Numerical simulation results showed that the two configurations can contribute to the frequency regulation during the transient disturbances by improving the RoCoF and the frequency nadir. However, integrating the features of dc voltage regulation in a VSM-controlled converter station, requires slower controller performance for the dc regulator and possibly increased dc-side capacitive energy storage.

References

[1] A. Ulbig, T. S. Borsche, G. Andersson, "Impact of Low Rotational Inertia on Power System Stability and Operation," in *Proceedings of the 19th World Congress of the International Federation of Automatic Control*, Cape Town, South Africa, August 24-29 2014, 8 pp.

[2] P. Tielens, "Operation and control of power systems with low synchronous inertia," PhD Thesis, KU Leuven, Belgium, Nov. 2017

[3] J. O'Sullivan, A. Rogers, D. Flynn, P. Smith, A. Mullane, M. O'Malley, "Studying the Maximum Instantaneous Non-Synchronous Generation in an Island System – Frequency Stability Challenges in Ireland," in *IEEE Transactions on Power Systems*, Vol. 29, No. 6, November 2014, pp. 2943-2951

[4] M. Yu, A. Dyśko, C. Booth, A. Roscoe, J. Zhu, H. Urdal, "Investigations on the Constraints relating to Penetration of Non-Synchronous Generation (NSG) in Future Power Systems," in *Proceedings of the 2015 Protection, Automation and Control (PAC) World Conference*, Glasgow, UK, 29 June – 2 July 2015, 9 pp.

[5] Y. Wang, V. Silva, M. Lopez-Botet-Zulueta, "Impact of high penetration of variable generation on frequency dynamics in the continental Europe interconnected system," in *IET Renewable Power Generation*, Vol. 10, No. 1, January 2016, pp. 10-16

[6] Statnett, Fingrid, Energinet.dk, Svenska Kraftnät, "Challenges and Opportunities for the Nordic Power System," August 2016,

[7] Booth, G. P. Adam, A. J. Roscoe, C. G. Bright, "Inertia Emulation Control Strategy for VSC-HVDC Transmission Systems," in *IEEE Trans.s on Power Systems*, Vol. 28, No. 2, May 2013, pp. 1277-1287

[8] J. Zhu, J. M. Guerrero, W. Hung, C. D. Booth, G. P. Adam, "Generic inertia emulation controller for multi-terminal voltage-source-converter high voltage direct current systems," in *IET Renewable Power Generation*, Vol. 8, No. 7, September 2014 pp. 740-748

[9] K. Rouzbehi, W. Zhang, J. I. Candela, A. Luna, P. Rodriguez, "Unified reference controller for flexible primary control and inertia sharing in multi-terminal voltage source converter-HVDC grids," in *IET Gen., Trans.& Distr.*, Vol. 11. No. 3, Feb. 2017, pp.750-758

[10] E. Rakhshani, P. Rodríguez, "Inertia Emulation in AC/DC Interconnected Power Systems Using Derivative Technique Considering Frequency Measurement Effects," in *IEEE Transactions on Power Systems*, Vol. 32, No. 5, September 2017, pp. 3338-3351

[11] W. Zhang, K. Rouzbehi, A. Luna, G. B. Gharehpetian, P. Rodriguez, "Multi-terminal HVDC grids with inertia mimicry capability," in *IET Renewable Power Generation*, Vol. 10, No. 6, July 2016, pp. 752-760

[12] R. Hesse, D. Turschner, H.-P. Beck, "Micro grid stabilization using the Virtual Synchronous Machine (VISMA)," in *Proceedings of the International Conference on Renewable Energies and Power Quality*, ICREPQ'09, Valencia, Spain, 15-17 April 2009, 6 pp.

[13] K. Sakimoto, Y. Miura, T. Ise, "Stabilization of a power system with a distributed generator by a virtual synchronous generator function," in *Proceedings of the 8th International Conference on Power Electronics – ECCE Asia*, Jeju, Korea, 30 May- 3 June 2011, 8 pp.

[14] Q.-C. Zhong, G. Weiss, "Synchronverters: Inverters That Mimic Synchronous Generators," *IEEE Transactions on Industrial Electronics*, vol. 58, no. 4, April 2011, pp. 1259-1267

[15] S. D'Arco, J. A. Suul, "Virtual Synchronous Machines – Classification of Implementations and Analysis of Equivalence to Droop Controllers for Microgrids," in *Proceedings of IEEE PowerTech Grenoble 2013*, Grenoble, France, 16-20 June 2013, 7 pp.

[16] B. Peng, X. Yin, J. Shen, J. Wang, "Application of Virtual Synchronization Control Strategy in MMC based VSC-HVDC System," in *Proceedings of the 2014 IEEE PES Asia-Pacific Power and Energy Engineering Conference*, APPEEC 2014, Kowloon, Hong Kong, 7-10 December 2014, 6 pp.

[17] M. Guan, W. Pan, J. Zhang, Q. Hao, J. Cheng, X. Zheng, "Synchronous Generator Emulation Control Strategy for Voltage Source Converter (VSC) Stations," in *IEEE Transactions on Power Systems*, Vol. 30, No. 6, November 2015, pp. 3093-3101

[18] S. D'Arco, G. Guidi, J. A. Suul, "Operation of a Modular Multilevel Converter Controlled as a Virtual Synchronous Machine," in *Proceedings of the International Power Electronics Conference*, IPEC 2018 ECCE Asia, Niigata, Japan, 20-24 May 2018, 8 pp.

[19] R. Aouini, B. Marinescu, K. B. Kilani, M. Elleuch, "Synchronverter-Based Emulation and Control of HVDC Transmission," in *IEEE Trans. on Power Systems*, Vol. 31, No. 1, January 2016, pp. 278-286

[20] R. Aouini, B. Marinescu, K. B. Kilani, M. Elleuch, "Stability improvement of the interconnection of weak AC zones by synchronverter-based HVDC link," in *Electric Power System Research*, Vol. 142, January 2017, pp. 112-124

[21] S. D'Arco, J. A. Suul, O. B. Fosso, "Small-Signal Modelling and Parametric Sensitivity of a Virtual Synchronous Machine," in *Proceedings of the 18th Power Systems Computation Conference*, PSCC 2014, Wrocław, Poland, 18-22 August 2014, 9 pp.

[22] J. Peralta, H. Saad, S. Dennetiére, J. Mahseredjian S. Nguefeu, "Detailed and averaged models for a 401-level MMC-HVDC system" *IEEE Trans. on Power Del.* Vol 27 No. 3 July 2012, pp.1501-1508

[23] S. D'Arco, G. Guidi, and J. A. Suul. "Embedded limitations and protections for droop-based control schemes with cascaded loops in the synchronous reference frame" *In proceedings of the 2014 Power Electronics Conference,* IPEC-Hiroshima 2014-ECCE-ASIA, 8 pp.

[24] C. Bajracharya, M. Molinas, J. A. Suul, T. M. Undeland, "Understanding of tuning techniques of converter controllers for VSC-HVDC." *Nordic Workshop on Power and Industrial Electronics,* NORPIE 2008, Espoo, Finland, 9-11 June 2008, 2008, 8 pp.

[25] S. D'Arco, J. A. Suul, O. B. Fosso, "Control System Tuning and Stability Analysis of Virtual Synchronous Machines," in *Proceeding of the 2013 IEEE Energy Conversion Congress and Exposition*, ECCE 2013, Denver, CO, USA, 15-19 Sept. 2013, 2013, pp. 2664-2671

[26] Callavik, Magnus, Peter Lundberg, and O. Hansson. "NORDLINK Pioneering VSC-HVDC interconnector between Norway and Germany." *ABB White Paper,* 2015

[27] Nexans, "NordLink HVDC interconnector between Norway and Germany will use Nexans' subsea power cable".

[28] F. Palombi, "HVDC Inertia Support – Inertia Emulation Control Strategy for VSC-HVDC Transmission Systems," MSc. Thesis, Politecnico di Milano, Italy, April 2019

This is the accepted version of an article published in 2019 IEEE Milan PowerTech
http://dx.doi.org/10.1109/PTC.2019.8810855